Malaysian Journal of Mathematical Sciences 20(1): 347–375 (2026)
https://doi.org/10.47836/mjms.20.1.17

Malaysian Journal of Mathematical Sciences

Journal homepage: https://mjms.upm.edu.my

Incorporating Memory Effects in the Caputo-Fabrizio Framework into a Predator-Prey Model with Structured Prey Dynamics

Sonowal, B. [1], Paul, R.* [1], Hazarika, P. J. [1], and Dutta, T. K. [2]

[1] *Department of Mathematics, Gauhati University, Guwahati-781014, Assam, India*
[2] *Department of Mathematics, Assam Don Bosco University, Guwahati-782402, Assam, India*

E-mail: ranupaul1984@gauhati.ac.in
**Corresponding author*

Received: 14 March 2025
Accepted: 13 July 2025

Abstract

This study introduces a predator-prey fishery model possessing a distinctive structural composition, featuring a single-stage predator population alongside a two-stage prey population dynamic. Additionally, the model considers harvesting efforts targeting the mature prey and predator populations. The novelty of this work lies in the incorporation of a biologically realistic two-stage prey structure within a fractional-order framework, along with the use of non-singular Caputo-Fabrizio derivatives, which allows for more accurate modeling of memory-dependent processes in ecological systems. To confirm the biological relevance of the proposed model, we first establish the existence and uniqueness of its solution. All equilibrium points of the system are determined and identified. Furthermore, the stability of the system, both locally and globally, is analyzed by employing the Jacobian matrix for system linearization and utilizing the Lyapunov direct approach for a detailed assessment. Lastly, numerical simulations are provided to support the analytical results, along with a graphical analysis of the system's behavior. The numerical simulations are performed employing the three-step Adam-Bashforth technique for fractional-order systems within the Caputo-Fabrizio framework.

Keywords: Caputo-Fabrizio fractional operator; predator-prey; biological equilibria; Lyapunov global stability.

1 Introduction

Marine biology is the study of marine animals, their behavior, and their interactions with the environment. A key objective of marine biology is to understand how oceanic phenomena influence the distribution of organisms. A key focus in studying the dynamics of marine ecosystems is gaining a deeper understanding of food chains and predator-prey relationships. Marine species play a vital role in the oxygen cycle and help regulate Earth's temperature. However, the excessive and uncontrolled harvesting of marine fish has the potential to drive many fish species to extinction. Another area of study in marine biology is the impact of various types of pollution on marine fish and plant life. This includes the effects of fertilizer and pesticide runoff from land-based sources, oil spills from tankers, and sedimentation caused by coastal construction projects. Additionally, the past 50 years have seen a significant growth in the human population and remarkable technological advancements. As a result, the global fish population has declined significantly.

The evolving relationships between predators and their prey in ecological systems are among the most intriguing topics in mathematical ecology. Various factors contribute to shaping the behavior of predator-prey models, including mortality rates, environmental conditions, and competition among predator populations. A wide range of ecological models is now available to represent the real-world behavior of various prey-predator species, from logistic growth models [43] to Lotka-Volterra interaction models [24, 44]. The predator-prey model plays a crucial role in understanding population dynamics. Over the years, numerous predator-prey systems have been formulated and studied by ecologists and mathematicians [18, 40]. Jin and Rang [20] proposed a predator-prey model that includes memory effects and intra-species competition among predators to analyze the occurrence of Hopf bifurcation. A simple multispecies harvesting model with two competing species and a predator was proposed by Kar and Chaudhuri [21], where the predator's feeding rate increases linearly with prey density.

Shao and Kong [36] studied a predator-prey model with Beddington-DeAngelis functional response and multiple delays under both deterministic and stochastic environments to explore the system's dynamic behavior. In recent years, the theory of fractional calculus has progressed swiftly and offers great potential for applications across multiple domains [33, 39]. Balci [8] studied the effects of predation fear and its carry-over impact in a fractional-order prey-predator model incorporating prey refuge, highlighting how fear can reduce prey growth and alter predator-prey dynamics. Bhunia. et al [11] investigated a fractional-order prey-predator model with delay and harvesting, revealing how fractional dynamics and harvesting types influence stability and induce switching behavior. A discrete fractional-order prey-predator model with predator harvesting was analysed by Uddin et al. [41], demonstrating the occurrence of Neimark-Sacker and period-doubling bifurcations and applying chaos control methods.

Unlike the integer-order derivative, the fractional derivative accounts for the entire time span of a biological process. In this context, various studies have explored the application of fractional calculus in modeling infectious diseases and biological systems. For instance, in [42], the authors proposed a fractional tuberculosis model using the Caputo-Fabrizio derivative to analyze disease dynamics and derive stability results. Similarly, a generalized fractional COVID-19 model incorporating isolation and quarantine effects was developed and validated using real clinical data from China, demonstrating better agreement with observed cases compared to classical models in [9]. Furthermore, Singh et al. [37] examined the dynamics of tumor growth using the Caputo-Fabrizio fractal-fractional derivative, where existence, stability, and numerical solutions were established through fixed-point theory and nonlinear analysis. Many population systems exhibit long-term memory [16], an effect that is overlooked in integer-order population models. Consequently, fractional-order population models provide benefits that surpass those of traditional integer-order models [38]. By incorporating the Lyapunov direct approach and exploring generalized Mittag-Leffler stability in nonlinear systems of fractional order, the authors have made substantial contributions to the advancement of fractional population dynamics models [22]. Building on this, researchers have applied this approach to create and analyze several fractional population models. For instance, Javidi et al. [19] presented a prey-predator interaction model incorporating harvesting using fractional-order derivatives. Almatrafi et al. [6] studied a fractional-order predator-prey model with Gompertz prey growth, analyzing its stability, bifurcations, and chaos control through theoretical and numerical methods. Additionally, several studies have focused on disease models related to the fishing industry. Sahoo et al. [34] analyzed strategies for controlling diseases within a food chain model that incorporates substitute food sources. Ah et al. [2] examined how disease in prey and cannibalism in predators affect the balance between predators and prey.

Recently, researchers have incorporated the Allee effect into ecological models to capture critical population thresholds and explore complex dynamics such as bistability, extinction scenarios, and bifurcation behavior under various environmental and biological conditions. Researchers have extensively explored the Allee effect due to its significant influence on species survival and extinction dynamics, leading to insightful studies on population behavior under various ecological conditions. In this context, Almatrafi et al. [5] investigated a predator-prey model incorporating the Allee effect using the conformable fractional derivative. They analyzed the equilibrium stability, bifurcation behavior, and chaos control through hybrid control techniques and numerical simulations. Furthermore, Almatrafi et al. [4] analyzed a fractional-order predator-prey model with Allee effect using conformable derivatives and piecewise-constant approximation. They demonstrated that the system undergoes Neimark-Sacker and period-doubling bifurcations under specific conditions. In [10], the authors explored the dynamics of a fractional-order activator-inhibitor system using the conformable derivative, focusing on the stability of equilibria and identifying conditions under which Neimark-Sacker and period-doubling bifurcations emerge.

This study examines the intricate behavior of predator-prey relationships by incorporating a differential equation with a fractional-order derivative, providing an extended framework for the fishery model. We assume that the prey population consists of two age structures: (i) the immature or juvenile phase, and (ii) the mature or adult phase. Furthermore, we incorporate the memory effect employing a fractional-order derivative, serving as a substitute for the traditional first-order derivative, and incorporate the influence of previous biological activities on the current state of the population. In this direction, several studies have explored the role of fractional calculus in biological modeling. Nawaz et al. [27] proposed a Caputo fractional-order TB model incorporating immune and asymptomatic classes, analyzing existence, stability, and sensitivity, and highlighting their roles in disease control through numerical simulations. In [31], the authors developed a fractional-order eco-epidemic predator-prey model using both Caputo and Atangana-Baleanu derivatives, analyzing stability, bifurcation, and bistability, and highlighting differences in convergence behavior between the two approaches. The authors also studied a Caputo fractional-order SEIRV model with optimal control for COVID-19, using real data from India to analyze stability and demonstrating improved performance over integer-order models through numerical simulations [25].

Additionally, a fractional-order predator-prey model with constant prey refuge and nonlinear incidence was analyzed in [26], emphasizing the influence of fractional dynamics on system behavior, stability, and Hopf bifurcation in comparison to classical models. Based on the memory effect, the current population dynamics are influenced by all previous conditions retained in the system's memory. These conditions include prior knowledge of where to find food, where to seek protection, when to migrate, and other factors. Fractional derivatives can be categorized into various forms, including those characterized by singular kernels, notably the Riemann-Liouville derivative [7, 29] and the Caputo derivative [7, 29], which are fundamental concepts in fractional calculus. Additionally, some derivatives are characterized by non-singular kernels, such as the Atangana-Baleanu derivative [13, 30], and the Caputo-Fabrizio derivative [1]. This study employs the Caputo-Fabrizio derivative as it efficiently addresses the challenges posed by the singular kernels present in the Riemann-Liouville and classical Caputo formulations. Initially proposed by Caputo et al. [15], the Caputo-Fabrizio approach offers a refined perspective on fractional differentiation. Unlike traditional derivatives, the Caputo-Fabrizio derivative is based on an exponential kernel, which offers the advantage of not relying on a single kernel. The Caputo-Fabrizio fractional derivative is also capable of capturing intricate dynamic behaviors that are challenging to represent with conventional integer-order derivatives. By accounting for memory effects and long-range interactions, this framework enables a more accurate and detailed modeling of complex systems found in biology, physics, and beyond.

We begin by developing a mathematical model using basic integer-order differential equations from classical calculus. We then extend this model within a fractional framework using the Caputo-Fabrizio derivative. The novelty of this work lies in modeling the predator-prey dynamics with a two-stage prey structure within a fractional-order framework using the Caputo-Fabrizio fractional derivative, which introduces memory and non-local effects into the classical system. Unlike traditional integer-order models, this fractional approach captures the hereditary properties and influence of the past states on the current population dynamics of predators and prey (both immature and mature). Additionally, incorporating two different harvesting efforts - one for predators and one for mature prey - adds a more realistic management aspect to the system. This combination allows for a more accurate and flexible representation of ecological interactions and harvesting impacts, offering new insights into stability and long-term behavior under fractional dynamics.

This paper is structured as follows, with the remaining sections arranged in the following manner. Section 2 introduces the preliminaries of the Caputo-Fabrizio fractional derivative. Section 3 formulates the fishery model and discusses its boundedness. In Section 4, we examine the properties and analyze the Caputo-Fabrizio model. Section 5 examines the essential conditions for ensuring the existence and uniqueness of solutions in the fractional model. Section 6 focuses on determining the model's equilibrium points, while Section 7 investigates the local stability of the equilibrium points. Furthermore, in Section 8, a comprehensive analysis of the global stability of the system is presented, examining its behavior over time and under varying conditions. Section 9 is dedicated to presenting the numerical discretization process, detailing the methods used to approximate the model for computational analysis. Section 10 provides a detailed discussion of the key findings, offering insights into the implications and relevance of the results. Finally, Section 11 concludes the paper by summarizing the overall study and presenting our final observations and reflections on the article.

2 Preliminaries

In this part, we outline the essential theorems, properties, and definitions that form the foundation for analyzing the main results of the proposed predator-prey system. This study specifically focuses on utilizing integrals and the Caputo-Fabrizio derivative.

Definition 2.1. *The Riemann-Liouville fractional integral operator of order* κ *(where* $\kappa > 0$*) with lower* *limit* $h_1 \geq 0$ *is defined as follows:*

$$(J_t^\kappa)f(t) = \frac{1}{\Gamma(\kappa)} \int_{h_1}^{t} (t-\tau)^{\kappa-1} f(\tau)d\tau, \quad t > h_1, \tag{1}$$

$$(J_t^0)f(t) = f(t), \tag{2}$$

where $\Gamma(.)$ *refers to the Gamma function.*

Definition 2.2. (*Caputo and Fabrizio* [7]) *We consider the following fractional derivative for the function* $f : [0, +\infty] \to \mathbb{R}$ *according to Caputo-Fabrizio sense of order* κ*:*

$$D_t^\kappa f(t) = \frac{CF(\kappa)}{1-\kappa} \int_0^t f'(\tau) \exp\left[-\frac{\kappa}{1-\kappa}(t-\tau)\right] d\tau, \quad t > 0, \tag{3}$$

$$\text{or} \quad D_t^\kappa f(t) = \frac{1}{\phi(\kappa)} \int_0^t f'(\tau) \exp\left[-\mu_\kappa(t-\tau)\right] d\tau, \qquad t > 0, \tag{4}$$

where $\mu_\kappa = \dfrac{\kappa}{1-\kappa}$, $\phi(\kappa) = \dfrac{1-\kappa}{CF(\kappa)}$. *The function* $CF(\kappa)$ *serves as a normalization function, satisfying the conditions* $CF(0) = 1$ *and* $CF(1) = 1$, *where the order* κ *lies in the range* $(0, 1)$.

One benefit of this fractional derivative is its ability to remove the singularity linked to the Caputo fractional derivative, as noted by Kilbas et al. [7] *and Podlubny* [32]. *The following definition describes its related integral.*

Definition 2.3. (*Losada and Nieto* [23]) *We examine the following fractional integral derivative for the function* $f : [0, +\infty] \to \mathbb{R}$ *according to Caputo-Fabrizio sense of order* κ*, as follows:*

$$I_t^\kappa f(t) = \frac{2(1-\kappa)f(t)}{(2-\kappa)CF(\kappa)} + \frac{2\kappa}{(2-\kappa)CF(\kappa)} \int_0^t f(\tau)d\tau. \tag{5}$$

The following equation represents the application of the Laplace transform to solve fractional differential equations governed by the Caputo-Fabrizio fractional derivative [21]*:*

$$\mathcal{L}[D_t^\kappa f](s) = CF(\kappa)\frac{s\mathcal{L}(f) - f(0)}{s + \kappa(1-s)}, \tag{6}$$

where $\mathcal{L}(f)$ *denotes the function f's Laplace transform.*

Definition 2.4. (*Hattaf* [17]) *We define the weighted generalized fractional derivative of order* $0 \leq \kappa \leq 1$ *for a function f and weight function* w*, as described below:*

$$D_w^{\kappa,\beta} f(t) = \frac{1}{\phi(\kappa)} \cdot \frac{1}{w(\kappa)} \int_{h_1}^{t} (wf)'(s) E_\beta[-\mu_\kappa(t-\tau)^\beta] d\tau, \tag{7}$$

where the weight function w *belongs to* $C^1([h_1, h_2])$ *satisfying* $w > 0$ *and* $w' > 0$. *The definition of the related fractional integral is:*

$$I_{t,w}^{\kappa,\beta} f(t) = \phi(\kappa)f(t) + \psi(\kappa)I_{t,w}^{\beta} f(t), \tag{8}$$

where $I_{t,w}^{\beta}$ *denotes the weighted Riemann-Liouville fractional integral operator of order* β.

Theorem 2.1. (*Hattaf* [17]) *Let* $\kappa \in [0, 1), \beta > 0$. *Then,*

$$I_{t,w}^{\kappa,\beta}(D_{t,w}^{\kappa,\beta} f(t)) = f(t) - \left(\frac{w(h_1)}{w(t)} f(h_1)\right). \tag{9}$$

When we take $w(t)$=1 *and* $\beta = 1$, *we obtain the Caputo Fabrizio derivative, given by,*

$$(J_t^\kappa D_t^\kappa f)(t) = f(t) - f(h_1). \tag{10}$$

Lemma 2.1. (*Wang and Wang* [45]) *Assume that the variable $x \in \mathbb{R}^+$ is a continuous function that can be derived. Then, the connection shown below is true whenever $t > 0$,*

$$D_t^{\kappa}\left[x - x^* - x^* \ln\left(\frac{x}{x^*}\right)\right] \leq \left[1 - \frac{x}{x^*}\right] D_t^{\kappa} x. \tag{11}$$

This lemma is crucial to our research, particularly in establishing the global asymptotic stability of the non-trivial equilibrium point.

3 Model Formulation

In this research, we examine a predator-prey model with a single-stage predator and a two-stage prey interacting with each other. The following sections will outline the key concepts that guided the development of our basic mathematical model.

We begin our model by incorporating a predator population into the logistic growth model. Let $x(t)$ represents the population density of the predator at time t. The logistic function, first introduced by Belgian mathematician Verhulst [43] in 1838, describes the growth of the predator biomass $x(t)$ as follows:

$$\frac{dx}{dt} = rx\left(1 - \frac{x}{K}\right).$$

Here, the symbol r signifies the predator's intrinsic per capita growth rate, reflecting its inherent reproductive capacity, while K represents the environment's carrying capacity for the predator population. The carrying capacity signifies the highest population size that the environment can support, beyond which growth is no longer possible due to resource limitations. This implies that as the population size increases, the per capita growth rate diminishes, ultimately reaching zero when the population approaches the saturation point at size K.

The formulation of the predator population model is presented below:

$$\frac{dx}{dt} = rx\left(1 - \frac{x}{K}\right) - d_1 x - q_1 E_1 x.$$

Here, the term $d_1 x$ signifies the natural mortality of the predator, while $q_1 E_1 x$ represents the amount of predator biomass harvested at time t.

The logistic growth model for the immature and mature prey population is given by:

$$\begin{aligned}\frac{dy}{dt} &= sy\left(1 - \frac{y+z}{L}\right),\\ \frac{dz}{dt} &= m_1 y\left(1 - \frac{y+z}{L}\right).\end{aligned}$$

Here, at time t, $y(t)$ represents the biomass density of immature prey and $z(t)$ represents the biomass density of the mature prey. L denotes the carrying capacity of the prey population. The parameter s signifies the intrinsic per capita growth rate of the prey, whereas m_1 represents the maturation rate of the prey species.

Thus, the model for immature and mature prey is constructed as follows:

$$\frac{dy}{dt} = sy\left(1 - \frac{y+z}{L}\right) - m_1 y - d_2 y - c_1 xy,$$
$$\frac{dz}{dt} = m_1 y\left(1 - \frac{y+z}{L}\right) - c_2 xz - q_2 E_2 z.$$

Here, the term $m_1 y$ represents the immature species that attains maturity, $d_2 y$ represents the death rate of the immature prey species, $c_1 xy$ and $c_2 xy$ signify the functional response of the predator's grazing behavior, and $q_2 E_2 z$ represents the harvested mature prey biomass at time t.

Taking into account the above considerations, we demonstrate the following predator-prey model using a set of nonlinear ordinary differential equations as the framework:

$$\frac{dx}{dt} = rx\left(1 - \frac{x}{K}\right) - d_1 x - q_1 E_1 x, \tag{12}$$
$$\frac{dy}{dt} = sy\left(1 - \frac{y+z}{L}\right) - m_1 y - d_2 y - c_1 xy, \tag{13}$$
$$\frac{dz}{dt} = m_1 y\left(1 - \frac{y+z}{L}\right) - c_2 xz - q_2 E_2 z. \tag{14}$$

All the parameters are considered to be positive. Here we have considered that for the mature prey species, there is no natural mortality. Here, throughout our analysis, we assume that,

$$c_1 > c_2, s > m_1. \tag{15}$$

The predator species relies on the prey as its primary food source, and the process of converting consumed prey into predator biomass is incorporated into the predator's growth model. Equations (12)–(14) describe the overall dynamics of the predator-prey model and can be represented by the equation below:

$$\begin{aligned}
p(t) &= x + y + z,\\
\frac{dp}{dt} &= \frac{dx}{dt} + \frac{dy}{dt} + \frac{dz}{dt}\\
&= rx\left(1 - \frac{x}{K}\right) - d_1 x - q_1 E_1 x + sy\left(1 - \frac{y+z}{L}\right) - m_1 y - d_2 y - c_1 xy\\
&\quad + m_1 y(1 - \frac{y+z}{L}) - c_2 xz - q_2 E_2 z\\
&= (r - d_1 - q_1 E_1)x - \frac{r}{K}x^2 + sy - d_2 y - \left(\frac{s}{L} + \frac{m_1}{L}\right) y^2 - \left(\frac{s}{L} + \frac{m_1}{L}\right) yz\\
&\quad - c_1 xy - c_2 xz - q_2 E_2 z.
\end{aligned}$$

By further simplifying the calculations, we obtain,

$$\frac{dp}{dt} \leq rx - \frac{r}{K}x^2 + sy - q_2 E_2 z.$$

By adding the positive quantity ϕp, where ϕ is any positive quantity, we obtain,

$$\begin{aligned}
\frac{dp}{dt} + \phi p &\leq rx - \frac{r}{K}x^2 + sy - q_2 E_2 z + \phi(x + y + z)\\
&= (r + \phi)x - \frac{r}{K}x^2 + (s + \phi)y + (\phi - q_2 E_2)z.
\end{aligned}$$

Now, if we choose $\phi < q_2E_2$, then $\phi - q_2E_2 < 0$. Also, since $y \leq L$, it follows,

$$(s+\phi)y \leq (s+\phi)L.$$

Hence,

$$\begin{aligned}
\frac{dp}{dt} + \phi p &\leq -\frac{r}{K}\left[x^2 - \frac{K}{r}(r+\phi)x\right] + (s+\phi)L \\
&= -\frac{r}{K}\left[\left\{x - \left(\frac{r+\phi}{2}\right)\frac{K}{r}\right\}^2 - \left\{\left(\frac{r+\phi}{2}\right)\frac{K}{r}\right\}^2\right] + (s+\phi)L \\
&\leq \frac{r}{K}.\frac{K^2}{r^2}\left(\frac{r+\phi}{2}\right)^2 + sL + \phi L, \\
\frac{dp}{dt} + \phi p &= \frac{K}{r}\left(\frac{r+\phi}{2}\right)^2 + (s+\phi)L.
\end{aligned}$$

This implies,

$$\frac{dp}{dt} + \phi p \leq C, \quad \text{where} \quad C = \frac{K}{r}\left(\frac{r+\phi}{2}\right)^2 + (s+\phi)L.$$

Integrating gives,

$$p(t) \leq \frac{C}{\phi} + ce^{-\phi t}, \quad \text{where c is a constant.}$$

As $t \to \infty$, $e^{-\phi t} \to 0$. Therefore, $p(t) \to \frac{C}{\phi} = \frac{1}{\phi}\left[\frac{K}{r}\left(\frac{r+\phi}{2}\right)^2 + (s+\phi)L\right]$, which is a finite quantity.

Thus, the total dynamics of the differential model is bounded by a finite number, which motivates us to incorporate the memory effect into this differential model and study its dynamics.

4 Properties and Analysis of the Caputo-Fabrizio Model

This section examines the predator-prey fishery model (12)–(14) using the Caputo-Fabrizio derivative. Since population dynamics are influenced by past states, the memory effect is essential for capturing real ecological interactions. To account for this, we reformulate the model with a fractional differential approach in the Caputo-Fabrizio sense, ensuring a more accurate representation of predator-prey dynamics. Thus, the model in our entire study is

$$D_t^\kappa x = rx\left(1 - \frac{x}{K}\right) - d_1x - q_1E_1x, \tag{16}$$

$$D_t^\kappa y = sy\left(1 - \frac{y+z}{L}\right) - m_1y - d_2y - c_1xy, \tag{17}$$

$$D_t^\kappa z = m_1y\left(1 - \frac{y+z}{L}\right) - c_2xz - q_2E_2z, \tag{18}$$

where κ represents the fractional order with $0 < \kappa < 1$, and the initial condition of the fractional order model are $x(0) > 0, y(0) > 0$ and $z(0) > 0$ for all $t \geq 0$.

Theorem 4.1. *Given that* $x(0) > 0, y(0) > 0, z(0) > 0$, *for all* $t \geq 0$, *we show that the set* $\lambda = \{ (x, y, z) \in \mathbb{R}^3_+ \}$ *attracts all non-negative solutions of the fractional order system* (16)–(18).

We present the following lemma that is utilized to demonstrate Theorem 4.1.

Lemma 4.1. (*Odibat and Shawagfeh* [28]) *Suppose* $f(t) \in C[h_1, h_2]$ *and* ${D_t}^{\kappa} f(t) \in C(h_1, h_2]$ *for all* $0 < \kappa \leq 1$, *then we have* $f(t) = f(h_1) + \frac{1}{\Gamma(\kappa)} {D_t}^{\kappa} f(\zeta)(t - h_1)^{\kappa}$, *where* $h_1 \leq \zeta \leq t$, *for all* $t \in (h_1, h_2]$.

Proof. Based on Definition 2.1, from (1) and (2), we can deduce the following:

$$\begin{aligned}(J_t^{\kappa} D_t^{\kappa}) f(t) &= \frac{1}{\Gamma(\kappa)} \int_{h_1}^{t} (t - \tau)^{\kappa - 1} (D_t^{\kappa} f)(\tau) d\tau, \\ (J_t^{\kappa} D_t^{\kappa} f)(t) &= \frac{1}{\Gamma(\kappa)} (D_t^{\kappa}) f)(\zeta) \int_{h_1}^{t} (t - \tau)^{\kappa - 1} d\tau \\ &= \frac{1}{\Gamma(\kappa)} (D_t^{\kappa} f)(\zeta).(t - h_1)^{\kappa}, \quad \text{for} \quad 0 \leq \zeta \leq t. \end{aligned} \tag{19}$$

On the other hand, according to (1), we have

$$(J_t^{\kappa} D_t^{\kappa} f)(t) = f(t) - f(h_1). \tag{20}$$

So, from (19) and (20), we obtain Lemma 4.1. □

Remark 4.1. *Assume that* $g(x) \in C[h_1, h_2]$ *and* ${D_t}^{\kappa} g(x) \in C[h_1, h_2]$ *for* $0 < \kappa \leq 1$. *Thus, it follows from Lemma 4.1 that if* ${D_t}^{\kappa} g(x) \geq 0$ *for all* $x \in (h_1, h_2)$, *then* $g(x)$ *is non decreasing and if* ${D_t}^{\kappa} g(x) \leq 0$ *for all* $x \in (h_1, h_2)$, *then* $g(x)$ *is non increasing.*

Now, we establish Theorem 16.

Proof. Here, we show that λ is positively invariant by demonstrating that the non-negative orthant of the vector field points into λ for any hyperplane bounding. Thus, from the system (16)–(18), we have

$$D_t^{\kappa} x = 0, \quad \text{(on the line } x(t) = 0).$$

Since $x(0) \geq 0$, and using Remark 4.1, $x(t)$ is non-decreasing,

$$D_t^{\kappa} y = 0, \quad \text{(on the line } y(t) = 0).$$

Since $y(0) \geq 0$, and using Remark 4.1, $y(t)$ is non-decreasing,

$$\begin{aligned} D_t^{\kappa} z = m_1 y \left(1 - \frac{y}{L}\right) \geq 0, &\quad \text{(on the line } z(t) = 0), \\ \geq 0 \quad [\because y(t) \leq L]. \end{aligned}$$

$$\therefore z(t) \text{ is non-decreasing.}$$

Consequently, for $t \geq 0$, λ is positively invariant and serves as an attractor for all non-negative solutions of the system (16)–(18). □

5 Existence and Uniqueness of the Solution to the Fractional model

This section focuses on analyzing the fractional fishery model represented by (16)–(18). This section aims to identify the conditions that guarantee a unique and ecologically viable solution for the fishery model. For simplification, we consider,

$$\delta_1(x,t) = rx\left(1-\frac{x}{K}\right) - d_1x - q_1E_1x, \tag{21}$$

$$\delta_2(y,t) = sy\left(1-\frac{y+z}{L}\right) - m_1y - d_2y - c_1xy, \tag{22}$$

$$\delta_3(z,t) = m_1y\left(1-\frac{y+z}{L}\right) - c_2xz - q_2E_2z. \tag{23}$$

The following function spaces are established. The Banach space, consisting of all functions that remain continuous and differentiable over the interval $[0,g]$ and map to $\mathbb{R}$, is represented by $C([0,g],\mathbb{R})$, and $C_\kappa[0,g] = \{x : [0,g] -> \mathbb{R}, \text{ s.t. } D_t^\kappa \text{ x} \in C[0,g]\}$.

For simplicity, we consider the classical norm defined by $\|\delta\|_{C_K} = \sup_{t\in[0,g]} \mid \delta(t,x) \mid$. We use the following notation in the next section of the study in relation to the applied norm. We concentrate on the following fractional differential equation:

$$D_t^\kappa x = \delta_1(t,x), \quad D_t^\kappa y = \delta_2(t,y) \quad \text{and} \quad D_t^\kappa z = \delta_3(t,z).$$

In this section, Banach fixed-point theory is utilized as the analytical framework to investigate the existence and uniqueness of solutions for the fractional-order system.

Theorem 5.1. *Let the functions $\delta_1(x,t)$, $\delta_2(y,t)$, and $\delta_3(z,t)$ defined in (21)–(23) be continuous and satisfy Lipschitz conditions on the Banach space $C([0,g],\mathbb{R})$. Then, for sufficiently small $g > 0$, each δ_i defines a contraction mapping if,*

$$C_\kappa(g)\cdot\xi_i < 1, \quad \textit{for } i = 1,2,3,$$

where ξ_i is the Lipschitz constant of δ_i, and $C_\kappa(g)$ is the norm of the Caputo-Fabrizio integral operator over $[0,g]$.

Proof. We begin by transforming the fractional-order system into an equivalent integral form using the Caputo-Fabrizio fractional integral operator as defined in (3).

Accordingly, the system can be rewritten as:

$$\begin{aligned} x(t) &= x_0 + I_{CF}^\kappa\left(\delta_1(t,x)\right), \\ y(t) &= y_0 + I_{CF}^\kappa\left(\delta_2(t,y)\right), \\ z(t) &= z_0 + I_{CF}^\kappa\left(\delta_3(t,z)\right). \end{aligned}$$

We first show that δ_1 is Lipschitz continuous. Let $x_1, x_2 \in C([0,g],\mathbb{R})$. Then,

$$\begin{aligned} \|\delta_1(x_1,t) - \delta_1(x_2,t)\| &= \left\|(r-d_1-q_1E_1)(x_1-x_2) - \frac{r}{K}(x_1^2-x_2^2)\right\| \\ &= \left\|\left[r-d_1-q_1E_1-\frac{r}{K}(x_1+x_2)\right](x_1-x_2)\right\| \\ &\le \left(|r-d_1-q_1E_1| + \frac{r}{K}\|x_1+x_2\|\right)\|x_1-x_2\|. \end{aligned}$$

Assuming $\|x_i\| \leq M$ for $i = 1, 2$, we define the Lipschitz constant:

$$\xi_1 = |r - d_1 - q_1 E_1| + \frac{2rM}{K}.$$

Under this assumption, we obtain

$$\|\delta_1(x_1, t) - \delta_1(x_2, t)\| \leq \xi_1 \|x_1 - x_2\|,$$

which implies that $\delta_1$is Lipschitz continuous with Lipschitz constant ξ_1. Similarly, we can obtain that δ_2 and δ_3 are Lipschitz continuous with the corresponding Lipschitz constants ξ_2 and ξ_3.

We now define Picard's operator as:

$$\mathcal{T}[x](t) = x_0 + I^{\kappa}_{CF}\left(\delta_1(t, x)\right).$$

To analyze the contraction property of the operator, we begin by estimating the norm of the Caputo-Fabrizio integral operator. For any $f \in C([0, g], \mathbb{R})$, we consider the function $f(t) = 1$. Then, by the Caputo-Fabrizio integral (3), we have

$$I^{\kappa}_{CF} 1(t) = \frac{2(1-\kappa)}{(2-\kappa)\,\mathrm{CF}(\kappa)} + \frac{2\kappa}{(2-\kappa)\,\mathrm{CF}(\kappa)} \cdot t.$$

Taking the supremum norm over the interval $[0, g]$, we obtain

$$\|I^{\kappa}_{CF} 1\| = \sup_{t \in [0,g]} |I^{\kappa}_{CF} 1(t)| = \frac{2(1-\kappa)}{(2-\kappa)\,\mathrm{CF}(\kappa)} + \frac{2\kappa g}{(2-\kappa)\,\mathrm{CF}(\kappa)}.$$

We define this bound as:

$$C_\kappa(g) = \frac{2(1-\kappa)}{(2-\kappa)\,\mathrm{CF}(\kappa)} + \frac{2\kappa g}{(2-\kappa)\,\mathrm{CF}(\kappa)}.$$

Now, using the Lipschitz continuity of δ_1, we estimate the norm of the operator $\mathcal{T}$ as follows:

$$\begin{aligned}
\|\mathcal{T}[x_1] - \mathcal{T}[x_2]\| &= \|I^{\kappa}_{CF}\left(\delta_1(t, x_1) - \delta_1(t, x_2)\right)\| \\
&\leq \|I^{\kappa}_{CF}\| \cdot \|\delta_1(x_1, t) - \delta_1(x_2, t)\| \\
&\leq C_\kappa(g) \cdot \xi_1 \cdot \|x_1 - x_2\|.
\end{aligned}$$

Therefore, the operator $\mathcal{T}$ is a contraction if the following condition holds:

$$C_\kappa(g) \cdot \xi_1 < 1.$$

Therefore, by Banach's fixed point theorem, a unique fixed point $x(t)$ exists in $C([0, g], \mathbb{R})$. Similarly, for the functions δ_2 and δ_3, if the corresponding Lipschitz constants ξ_2 and ξ_3 satisfy $0 \leq C_\kappa(g) \cdot \xi_2, C_\kappa(g) \cdot \xi_3 < 1$, then the same type of argument applies. As a result, we can conclude that by Banach's fixed point theorem, unique fixed points $y(t)$ and $z(t)$ exists in $C([0, g], \mathbb{R})$. □

Theorem 5.2 (Uniqueness of Solutions). *Let $x_1(t)$, $x_2(t)$, $y_1(t)$, $y_2(t)$, $z_1(t)$, and $z_2(t)$ be solutions to the integral equations,*

$$\begin{aligned}
x(t) &= x_0 + I^{\kappa}_{CF}\left(\delta_1(t, x)\right), \\
y(t) &= y_0 + I^{\kappa}_{CF}\left(\delta_2(t, y)\right), \\
z(t) &= z_0 + I^{\kappa}_{CF}\left(\delta_3(t, z)\right),
\end{aligned}$$

where each δ_i is Lipschitz continuous with constant ξ_i, and the Caputo-Fabrizio operator norm satisfies,

$$C_\kappa(g) \cdot \xi_i < 1, \quad \textit{for } i = 1, 2, 3.$$

Then, $x_1(t) = x_2(t)$, $y_1(t) = y_2(t)$, and $z_1(t) = z_2(t)$ for all $t \in [0, g]$; that is, the solution to each component is unique.

Proof. Since both x_1 and x_2 are solutions of the integral equation, we have

$$x_1(t) = x_0 + I^\kappa_{CF}\left(\delta_1(t, x_1(t))\right),$$
$$x_2(t) = x_0 + I^\kappa_{CF}\left(\delta_1(t, x_2(t))\right).$$

Subtracting the above two equations yields

$$x_1(t) - x_2(t) = I^\kappa_{CF}\left(\delta_1(t, x_1) - \delta_1(t, x_2)\right).$$

Taking norms on both sides and applying the norm estimate for the Caputo-Fabrizio integral operator, we get,

$$\|x_1 - x_2\| \leq \|I^\kappa_{CF}\left(\delta_1(t, x_1) - \delta_1(t, x_2)\right)\| \leq C_\kappa(g) \cdot \|\delta_1(t, x_1) - \delta_1(t, x_2)\| \leq C_\kappa(g) \cdot \xi_1 \cdot \|x_1 - x_2\|,$$

which implies that,

$$[1 - C_\kappa(g) \cdot \xi_1] \cdot \|x_1 - x_2\| \leq 0.$$

Since $C_\kappa(g) \cdot \xi_1 < 1$, it must satisfy that $\|x_1 - x_2\| = 0$, which implies,

$$x_1(t) = x_2(t), \quad \text{for all } t \in [0, g].$$

Similarly, the same steps can be repeated for the $y(t)$ and $z(t)$ components under the assumptions $C_\kappa(g) \cdot \xi_2 < 1$ and $C_\kappa(g) \cdot \xi_3 < 1$, respectively. This proves that $y_1(t) = y_2(t)$ and $z_1(t) = z_2(t)$ on the interval $[0, g]$, thereby ensuring uniqueness of the full solution vector $(x(t), y(t), z(t))$. ☐

6 Biological Equilibria

Biological equilibria are essentially the steady-state points of our model. Hence, the equilibrium points of the system (12)–(14) are determined by solving the following set of simultaneous equations:

$$\frac{dx}{dt} = rx\left(1 - \frac{x}{K}\right) - d_1x - q_1E_1x = 0, \tag{24}$$

$$\frac{dy}{dt} = sy\left(1 - \frac{y+z}{L}\right) - m_1y - d_2y - c_1xy = 0, \tag{25}$$

$$\frac{dz}{dt} = m_1y\left(1 - \frac{y+z}{L}\right) - c_2xz - q_2E_2z = 0. \tag{26}$$

The equilibrium point $E_0 = (0, 0, 0)$ represents the initial equilibrium, indicating the extinction of both the predator and the immature and mature prey. This equilibrium point is always present. The second equilibrium point $E_1^*(\bar{x}, 0, 0)$ represents the state where only predator biomass is present, with no prey biomass. The existence of this equilibrium point is given by the condition:

$$r - d_1 - q_1E_1 > 0.$$

The existence of the equilibrium point $E_2^*(0, \bar{y}, \bar{z})$, which denotes the absence of the predator and the presence of only the prey population, is established in the following theorem.

Theorem 6.1. *The equilibrium point* $E_2^*(0, \bar{y}, \bar{z})$ *exist if it satisfies the condition:* $s > m_1 + d_2 > 0$.

Proof. From the governing equation (25), we have

$$y = 0 \quad \text{or} \quad y + z = \frac{L}{s}(s - m_1 - d_2 - c_1 x).$$

$$\text{If} \quad x = 0, \quad \text{then} \quad y + z = \frac{L}{s}(s - m_1 - d_2). \tag{27}$$

If $s - m_1 - d_2 < 0$, then $y + z$ does not exist. Therefore, for a non-zero equilibrium point to exist, the condition $s - m_1 - d_2 > 0$ must be satisfied.

Then, from (26), we have

$$z = \frac{m_1 y}{q_2 E_2}\left[1 - \frac{1}{s}(s - m_1 - d_2)\right]. \tag{28}$$

Using (28) in (27), we have

$$y = \frac{\frac{L}{s}(s - m_1 - d_2)}{1 + \frac{m_1}{q_2 E_2}\left(1 - \frac{1}{s}(s - m_1 - d_2)\right)}.$$

Hence, we have the equilibrium point $E_2^*(0, \bar{y}, \bar{z})$, where

$$x = 0, \quad \bar{y} = \frac{\frac{L}{s}(s - m_1 - d_2)}{1 + \frac{m_1}{q_2 E_2}\left(1 - \frac{1}{s}(s - m_1 - d_2)\right)} \quad \text{and} \quad \bar{z} = \frac{m_1 y}{q_2 E_2}\left[1 - \frac{1}{s}(s - m_1 - d_2)\right].$$

□

Theorem 6.2. *For the existence of the coexisting equilibrium point* $E^*(x^*, y^*, z^*)$ *it must satisfy the conditions:*

1. $r - d_1 - q_1 E_1 > 0$.
2. $s - m_1 - d_2 > c_1 x^* + \dfrac{s z^*}{L} > 0$.
3. $c_2 x + q_2 E_2 > 0$.

Proof. From the governing equations, we analyze the equilibrium conditions as follows:

- Equation (24) gives $x = 0$ or $x = \dfrac{K}{r}(r - d_1 - q_1 E_1)$.
- For $x \neq 0$, we have $x = \dfrac{K}{r}(r - d_1 - q_1 E_1) = x^*(say)$.

- From (25), we have $y = 0$ or $y^* = \dfrac{L}{s}\left(s - m_1 - d_2 - c_1 x^* - \dfrac{sz^*}{L}\right)$.
- From (26), we have $z = 0$ or $z^* = \dfrac{m_1 y^*(L - y^*)}{L(c_2 x^* + q_2 E_2)}$.

At equilibrium, $z^* \geq 0$, so the denominator $c_2 x^* + q_2 E_2 > 0$. Additionally, z^* is feasible when $y^*(L - y^*) > 0$, which is satisfied naturally as $0 < y^* < L$. Thus, to ensure the existence of the equilibrium point $E^*(x^*, y^*, z^*)$ the following feasibility conditions must hold:

1. $r - d_1 - q_1 E_1 > 0$.
2. $s - m_1 - d_2 > c_1 x^* + \dfrac{sz^*}{L} > 0$.
3. $c_2 x + q_2 E_2 > 0$.

Hence, the system has a co-existing equilibrium point denoted as $E^*(x^*, y^*, z^*)$. □

7 Analysis of the Local Stability of Equilibrium Points

The local stability of the non-linear systems involving fractional derivative provides insights into the behaviour of solutions near the equilibrium points. The Caputo-Fabrizio derivative, characterized by a non-singular and exponential kernel, offers an advantage over classical definitions by avoiding singularities and simplifying certain analytical procedures. In this context, local stability is typically assessed by linearizing the system around its equilibrium points and examining the signs of the eigenvalues of the corresponding Jacobian matrix J. The Routh-Hurwitz criterion is used to check if all roots of the characteristic equation have negative real parts, confirming local stability of the equilibrium. If all eigenvalues are negative real numbers, they satisfy the condition $|\arg(\lambda)| > \dfrac{\kappa\pi}{2}$, thereby ensuring local stability [12, 35]. We define the fractional differential equation as follows:

$$D_t^{\kappa} x = u(x, y, z), \quad D_t^{\kappa} y = v(x, y, z) \quad \text{and} \quad D_t^{\kappa} z = w(x, y, z). \tag{29}$$

The equations provided by the following relationships are satisfied by the equilibrium points of (29):

$$u(x_{eq}, y_{eq}, z_{eq}) = 0, \quad v(x_{eq}, y_{eq}, z_{eq}) = 0 \quad \text{and} \quad w(x_{eq}, y_{eq}, z_{eq}) = 0, \tag{30}$$

where (x_{eq}, y_{eq}, z_{eq}) stands for the fractional model's equilibrium point. We obtain four distinct equilibrium points with one element null following resolution.

Theorem 7.1. *The point E_0 is an unstable saddle equilibrium point.*

Proof. The Jacobian matrix evaluated at the trivial equilibrium point $E_0(0, 0, 0)$ is given by:

$$J(E_0) = \begin{pmatrix} r - d_1 - q_1 E_1 & 0 & \\ 0 & s - m_1 - d_2 & 0 \\ 0 & m_1 & -q_2 E_2 \end{pmatrix}.$$

The eigenvalues at the equilibrium point $E_0(0,0,0)$ are $\lambda_1 = r - d_1 - q_1E_1$, $\lambda_2 = s - m_1 - d_2$ and $\lambda_3 = -q_2E_2$. Here, one of the eigenvalues, λ_3, is negative. Thus, $|\arg(\lambda_3)| > \dfrac{\kappa\pi}{2}$ is satisfied. For the existence of the nonzero equilibrium point, conditions $r - d_1 - q_1E_1 > 0$ and $s - m_1 - d_2 > 0$ must be satisfied, leading to the conclusion that the equilibrium point must imply $\lambda_1 > 0$ and $\lambda_2 > 0$. As a result, it satisfies the condition $|\arg(\lambda_1)| < \dfrac{\kappa\pi}{2}$ and $|\arg(\lambda_2)| < \dfrac{\kappa\pi}{2}$. Thus, E_0 is an unstable saddle equilibrium point. □

Theorem 7.2. *If* $s - m_1 - d_2 < c_1\bar{x}$ *and if* $r - d_1 - q_1E_1 < \dfrac{2r\bar{x}}{K}$, *then* E_1^* *is locally asymptotically stable. The equilibrium point* E_1^* *is a saddle point if one of the following conditions holds:*

1. $s - m_1 - d_2 > c_1\bar{x}$ *and if* $r - d_1 - q_1E_1 < \dfrac{2r\bar{x}}{K}$, *or*
2. $s - m_1 - d_2 < c_1\bar{x}$ *and if* $r - d_1 - q_1E_1 > \dfrac{2r\bar{x}}{K}$.

Proof. The Jacobian matrix evaluated at the equilibrium point $E_1^*(\bar{x},0,0)$, which corresponds to the absence of prey biomass and the presence of only predator biomass is given by:

$$J(E_1^*) = \begin{pmatrix} -\dfrac{2r\bar{x}}{K} + (r - d_1 - q_1E_1) & 0 & 0 \\ 0 & s - m_1 - d_2 - c_1\bar{x} & 0 \\ 0 & m_1 & -c_2\bar{x} - q_2E_2 \end{pmatrix}.$$

The eigenvalues at the equilibrium point $E_1^*(\bar{x},0,0)$ are $\lambda_1 = -\dfrac{2r\bar{x}}{K} + (r_1 - d_2 - q_1E_1)$, $\lambda_2 = s - m_1 - d_2 - c_1\bar{x}$ and $\lambda_3 = -c_2\bar{x} - q_2E_2$. Since λ_3 is negative, it follows that the argument of λ_3 satisfies $|\arg(\lambda_3)| > \dfrac{\kappa\pi}{2}$. Therefore, the stability is validated by the argument of λ_3. Now, if $s - m_1 - d_2 < c_1\bar{x}$, then subsequently λ_2 has a negative sign that impacts $|\arg(\lambda_2)| > \dfrac{\kappa\pi}{2}$. If $r - d_1 - q_1E_1 < \dfrac{2r\bar{x}}{K}$, then $\lambda_1 < 0$, which implies that it satisfies the condition $|\arg(\lambda_1)| > \dfrac{\kappa\pi}{2}$. Therefore, the equilibrium point $E_1^*(\bar{x},0,0)$ exhibits local asymptotic stability if and only if this stated condition is satisfied; otherwise, it behaves as a saddle point. □

Theorem 7.3. *If* $\Delta = 18\beta_1\beta_2\beta_3 + (\beta_1\beta_2)^2 - 4\beta_3\beta_1^3 - 4\beta_2^3 - 27\beta_3^3$, *then the equilibrium point* $E_2^*(0,\bar{y},\bar{z})$ *is locally asymptotically stable if atleast one of the following conditions is satisfied:*

1. $\Delta > 0$, $\beta_1 > 0$, $\beta_3 > 0$ *and* $\beta_1\beta_2 > \beta_3$.
2. $\Delta < 0$, $\beta_1 \geq 0$, $\beta_2 \geq 0$, $\beta_3 > 0$ *and* $\kappa < \dfrac{2}{3}$.
3. $\Delta < 0$, $\beta_1 < 0$, $\beta_2 < 0$ *and* $\kappa > \dfrac{2}{3}$.
4. $\Delta < 0$, $\beta_1 > 0$, $\beta_2 > 0$, $\beta_1\beta_2 = \beta_3$ *for all* $0 < \kappa < 1$.

Proof. The Jacobian matrix at the equilibrium point $E_2^*(0, \bar{y}, \bar{z})$, which represents the scenario with the presence of immature and mature prey but no predator biomass, is given by:

$$J(E_2^*) = \begin{pmatrix} a_{11} & a_{12} & a_{13} \\ a_{21} & a_{22} & a_{23} \\ a_{31} & a_{32} & a_{33} \end{pmatrix},$$

where

$$\begin{aligned} a_{11} &= -r + d_1 + q_1E_1, & a_{12} &= 0, & a_{13} &= 0, \\ a_{21} &= c_1\bar{y}, & a_{22} &= \frac{2s\bar{y}}{L} - s + \frac{s\bar{z}}{L} + m_1 + d_2, & a_{23} &= \frac{s\bar{y}}{L}, \\ a_{31} &= c_2\bar{z}, & a_{32} &= \frac{2m_1\bar{y}}{L} - m_1 + \frac{m_1\bar{z}}{L}, & a_{33} &= \frac{m_1\bar{y}}{L} + q_2E_2. \end{aligned}$$

The characteristic polynomial corresponding to the above Jacobian matrix is

$$\lambda^3 + \beta_1\lambda^2 + \beta_2\lambda + \beta_3 = 0,$$

where the parameters are given by:

$$\begin{aligned} \beta_1 &= r - d_1 - q_1E_1 + s - m_1 - d_2 - q_2E_2 - (2s + m_1)\frac{\bar{y}}{L} - \frac{s\bar{z}}{L}, \\ \beta_2 &= (r - d_1 - q_1E_1 - q_2E_2)\left(s - m_1 - d_2 - (2\bar{y} + \bar{z})\frac{s}{L}\right) + (m_1 + d_2)\frac{m_1\bar{y}}{L} \\ &\quad - (r - d_1 - q_1E_1)\left(\frac{m_1\bar{y}}{L} + q_2E_2\right), \\ \beta_3 &= (r - d_1 - q_1E_1)\left[(m_1 + d_2)\frac{m_1\bar{y}}{L} - \left(s - m_1 - d_2 - (2\bar{y} + \bar{z})\frac{s}{L}\right) q_2E_2\right]. \end{aligned}$$

Hence, based on the application of Proposition 1 in Ahmed et al. [3], we can confirm the validity of all of the propositions provided in Theorem 7.3. ☐

Theorem 7.4. *If* $\Delta = 18\gamma_1\gamma_2\gamma_3 + (\gamma_1\gamma_2)^2 - 4\gamma_3\gamma_1^3 - 4\gamma_2^3 - 27\gamma_3^2$, *then the equilibrium point* $E^*(x^*, y^*, z^*)$ *is locally asymptotically stable if atleast one of the following conditions is satisfied:*

1. $\Delta > 0, \gamma_1 > 0, \gamma_3 > 0$ *and* $\gamma_1\gamma_2 > \gamma_3$.
2. $\Delta < 0, \gamma_1 \geq 0, \gamma_2 \geq 0, \gamma_3 > 0$ *and* $\kappa < \frac{2}{3}$.
3. $\Delta < 0, \gamma_1 < 0, \gamma_2 < 0$ *and* $\kappa > \frac{2}{3}$.
4. $\Delta < 0, \gamma_1 > 0, \gamma_2 > 0, \gamma_1\gamma_2 = \gamma_3$ *for all* $0 < \kappa < 1$.

Proof. The Jacobian matrix at the co-existing equilibrium point $E^*(x^*, y^*, z^*)$ is

$$J(E^*) = \begin{pmatrix} b_{11} & b_{12} & b_{13} \\ b_{21} & b_{22} & b_{23} \\ b_{31} & b_{32} & b_{33} \end{pmatrix},$$

where

$$b_{11} = \frac{2rx^*}{K} - r + d_1 + q_1E_1, \quad b_{12} = 0, \quad b_{13} = 0,$$
$$b_{21} = c_1y^*, \quad b_{22} = \frac{2sy^*}{L} + \frac{sz^*}{L} - s + m_1 + d_2 + c_1x^*, \quad b_{23} = \frac{sy^*}{L},$$
$$b_{31} = c_2z^*, \quad b_{32} = \frac{2m_1y^*}{L} + \frac{m_1z^*}{L} - m_1, \quad b_{33} = \frac{m_1y^*}{L} + c_2x^* + q_2E_2.$$

The characteristic polynomial corresponding to the above Jacobian matrix is

$$\lambda^3 + \gamma_1\lambda^2 + \gamma_2\lambda + \gamma_3 = 0,$$

where the parameters are given by:

$$\gamma_1 = -\frac{2rx^*}{K} + r - d_1 - q_1E_1 - \frac{2sy^*}{L} - \frac{sz^*}{L} + s - m_1 - d_2 - c_1x^* - \frac{m_1y^*}{L} - c_2x^* - q_2E_2,$$
$$\gamma_2 = \left(\frac{2sy^*}{L} + \frac{sz^*}{L} - s + m_1 + d_2 + c_1x^*\right)\left(\frac{m_1y^*}{L} + c_2x^* + q_2E_2 + \frac{2rx^*}{K} - r + d_1 + q_1E_1\right)$$
$$- \frac{sy^*}{L}\left(\frac{2m_1y^*}{L} + \frac{m_1z^*}{L} - m_1\right) + \left(\frac{2rx^*}{K} - r + d_1 + q_1E_1\right)\left(\frac{m_1y^*}{L} + c_2x^* + q_2E_2\right),$$
$$\gamma_3 = \left(\frac{2rx^*}{K} - r + d_1 + q_1E_1\right)\left[\frac{m_1^2y^*}{L} + \frac{d_2m_1y^*}{L} + \frac{c_1m_1x^*y^*}{L} + (c_2x^* + q_2E_2)\times\right.$$
$$\left.\left(\frac{2sy^*}{L} + \frac{sz^*}{L} - s + m_1 + d_2 + c_1x^*\right)\right].$$

Hence, based on the application of Proposition 1 in Ahmed et al. [3], we can confirm the validity of all of the propositions provided in Theorem 7.4. □

8 Analysis of Lyapunov Global Stability

In this section, we employ the Lyapunov function method to analyze the stability of the system as shown in [35, 14]. To study the global stability of the non-trivial co-existing equilibrium point, we propose a Lyapunov function defined as $Q(x, y, z) = Q_1(x) + Q_2(y) + Q_3(z)$, where

$$Q_1(x) = \left[x - x^* - x^* \ln\left(\frac{x}{x^*}\right)\right], \tag{31}$$

$$Q_2(y) = \left[y - y^* - y^* \ln\left(\frac{y}{y^*}\right)\right], \tag{32}$$

$$Q_3(z) = \left[z - z^* - z^* \ln\left(\frac{z}{z^*}\right)\right]. \tag{33}$$

This function is valid for stability analysis because it is continuously differentiable and positive definite, with $Q(x, y, z) \geq 0$ for all positive x, y, z, and it equals zero if and only if $(x, y, z) = (x^*, y^*, z^*)$, the equilibrium point. These properties ensure that Q effectively measures the deviation from equilibrium, making it suitable for proving global stability of the system. Next, we utilize the Caputo-Fabrizio derivative on the Lyapunov function associated with (31),

$$\begin{aligned} D_t^\kappa Q_1(x) &\leq \left[1-\frac{x^*}{x}\right] D_t^\kappa x, \qquad [\text{using } (11)] \\ &\leq \left[\frac{x-x^*}{x}\right]\left[rx\left(1-\frac{x}{K}\right)-d_1x-q_1E_1x\right]. \end{aligned}$$

Furthermore, the equation above can be rewritten as follows at the non-trivial equilibrium point:

$$\begin{aligned} D_t^\kappa Q_1(x) &\leq \left[\frac{x-x^*}{x}\right]\left[rx\left(1-\frac{x}{K}\right)-d_1x-q_1E_1x\right] \\ &\leq \left[\frac{x-x^*}{x}\right]\left[r(x-x^*)-\frac{r(x^2-x^{*2})}{K}-d_1(x-x^*)-q_1E_1(x-x^*)\right] \\ &= (r-d_1-q_1E_1)\frac{(x-x^*)^2}{x}-\frac{r}{K}\frac{(x-x^*)^2(x+x^*)}{x} \\ &\leq \left(r-d_1-q_1E_1-\frac{r}{K}x^*\right)\frac{(x-x^*)^2}{x}. \end{aligned}$$

Now, to get $D_t^\kappa Q_1(x) \leq 0$, it must satisfy $E_1 \geq \frac{1}{q_1}\left(r-d_1-\frac{rx^*}{K}\right)$.

We proceed with the computations using the second and third equations of the predator -prey model. By applying the Caputo-Fabrizio derivative to the Lyapunov function (32)–(33), we obtain the following results:

$$\begin{aligned} D_t^\kappa Q_2(y)+D_t^\kappa Q_3(z) &\leq \left[1-\frac{y^*}{y}\right]D_t^\kappa y+\left[1-\frac{z^*}{z}\right]D_t^\kappa z \\ &\leq \left[\frac{y-y^*}{y}\right]\left[sy\left(1-\frac{y+z}{L}\right)-m_1y-d_2y-c_1xy\right]+\left[\frac{z-z^*}{z}\right]\times \\ &\quad \left[m_1y\left(1-\frac{y+z}{L}\right)-c_2xz-q_2E_2z\right] \\ &\leq \left[\frac{y-y^*}{y}\right]\left[s(y-y^*)-\frac{s}{L}(y^2-y^{*2})-\frac{s}{L}(yz-y^*z^*)-m_1(y-y^*)\right. \\ &\quad \left.-d_2(y-y^*)-c_1(xy-x^*y^*)\right]+\left[\frac{z-z^*}{z}\right]\left[m_1(y-y^*)-\frac{m_1}{L}(y^2-y^{*2})\right. \\ &\quad \left.-\frac{m_1}{L}(yz-y^*z^*)-c_2(xz-x^*z^*)-q_2E_2(z-z^*)\right], \\ D_t^\kappa Q_2(y)+D_t^\kappa Q_3(z) &\leq s\frac{(y-y^*)^2}{y}-\frac{s}{L}\cdot\frac{y^*(y-y^*)(z-z^*)}{y}-c_1\cdot\frac{y^*(x-x^*)(y-y^*)}{y} \\ &\quad +m_1\cdot\frac{(y-y^*)(z-z^*)}{z}-\frac{m_1}{L}\cdot\frac{(y+y^*)(y-y^*)(z-z^*)}{z} \\ &\quad -\frac{m_1}{L}\cdot\frac{z^*(y-y^*)(z-z^*)}{z}-c_2\cdot\frac{z^*(x-x^*)(z-z^*)}{z}-q_2E_2\cdot\frac{(z-z^*)^2}{z}. \end{aligned}$$

Consider a domain, $\Omega^* = \left\{(x,y,z)\middle|\dfrac{x}{x^*} > 1, \dfrac{y}{y^*} > 1, \dfrac{z}{z^*} > 1, \dfrac{y+z}{y^*+z^*} < 1\right\}$. Then, we have

$$\begin{aligned} D_t^\kappa Q_2(y) + D_t^\kappa Q_3(z) &\leq s\frac{(y-y^*)^2}{y} + m_1\frac{(y-y^*)(z-z^*)}{z} - q_2E_2\frac{(z-z^*)^2}{z} \\ &\leq s\frac{(z-z^*)^2}{y} + m_1\frac{(z-z^*)^2}{z} - q_2E_2\frac{(z-z^*)^2}{z} \\ &= \left(\frac{s}{y} + \frac{m_1}{z} - \frac{q_2E_2}{z}\right)(z-z^*)^2. \end{aligned}$$

Now, to ensure that $D_t^\kappa Q_2(y) + D_t^\kappa Q_3(z) \leq 0$, the following condition must be satisfied:

$$\frac{s}{y} + \frac{m_1}{z} - \frac{q_2E_2}{z} \leq 0, \quad \text{which follows that} \quad E_2 \geq \frac{m_1}{q_2}, \quad \text{as } 0 \leq z \leq L.$$

Finally, the expression below denotes the Caputo-Fabrizio derivative of the Lyapunov function Q concerning the trajectories governed by (16)–(18),

$$D_t^\kappa Q = D_t^\kappa Q_1(x) + D_t^\kappa Q_2(y) + D_t^\kappa Q_3(z) \leq 0.$$

From the existence of non-zero x, we have the condition $E_1 \leq \dfrac{r-d_1}{q_1}$. Thus, the harvesting effort of the predator must satisfy the condition:

$$\frac{1}{q_1}\left(r - d_1 - \frac{rx^*}{K}\right) \leq E_1 \leq \frac{r-d_1}{q_1}. \tag{A}$$

Moreover, the harvesting effort of the prey must satisfy the condition:

$$E_2 \geq \frac{m_1}{q_2}. \tag{B}$$

Therefore, when the conditions specified in (A) and (B) are satisfied, the interior equilibrium point is globally asymptotically stable, indicating that all trajectories of the system eventually converge to this equilibrium.

9 Numerical Discretization

The numerical simulation of the model system (16)–(18) has been generated using the three-step Adams-Bashforth schemes, as presented in [29]. A comprehensive examination of the fractional fishery model will be performed utilizing the solutions. From the definition of the Caputo-Fabrizio operator, we obtain:

$$\begin{aligned} D_t^\kappa u(t) &= \frac{CF(\kappa)}{1-\kappa}\int_0^t u'(\tau)e^{-\frac{\kappa}{1-\kappa}(t-\tau)}d\tau, \\ f(t,u(t)) &= \frac{CF(\kappa)}{1-\kappa}\int_0^t u'(\tau)e^{-\frac{\kappa}{1-\kappa}(t-\tau)}d\tau, \quad [\text{Here, } f(t,u(t)) = D_t^\kappa u(t)], \\ \int_0^t u'(\tau)e^{-\frac{\kappa}{1-\kappa}(t-\tau)}d\tau &= \frac{1-\kappa}{CF(\kappa)}f(t,u(t)), \\ \left[e^{-\frac{\kappa}{1-\kappa}(t-\tau)}u(\tau)\right]_0^t - \int_0^t \left(\frac{\kappa}{1-\kappa}\right)&e^{-\frac{\kappa}{1-\kappa}(t-\tau)}u(\tau)d\tau = \frac{1-\kappa}{CF(\kappa)}f(t,u(t)), \end{aligned}$$

$$u(t) - e^{-\frac{\kappa}{1-\kappa}(t)}u(0) = \frac{1-\kappa}{CF(\kappa)}f(t,u(t)) + \frac{\kappa}{CF(\kappa)}\int_0^t f(\tau,u(\tau))d\tau,$$

$$u(t) - u(0) = \frac{1-\kappa}{CF(\kappa)}f(t,u(t)) + \frac{\kappa}{CF(\kappa)}\int_0^t f(\tau,u(\tau))d\tau.$$

$\because$ Caputo-Fabrizio derivative $D_t^{\kappa}u(t)$ i.e. $f(t,u(t))$ is a linear transformation.

Upon discretization, the following recurrence relation is derived:

$$u(t_{n+1}) - u(0) = \frac{1-\kappa}{CF(\kappa)}f(t_n,u(t_n)) + \frac{\kappa}{CF(\kappa)}\int_0^{t_{n+1}} f(t,u(t))dt, \tag{34}$$

$$u(t_n) - u(0) = \frac{1-\kappa}{CF(\kappa)}f(t_{n-1},u(t_{n-1})) + \frac{\kappa}{CF(\kappa)}\int_0^{t_n} f(t,u(t))dt. \tag{35}$$

The difference between (34) and (35) gives,

$$u(t_{n+1}) - u(t_n) = \frac{1-\kappa}{CF(\kappa)}\{f(t_n,u_n) - f(t_{n-1},u_{n-1})\} + \frac{\kappa}{CF(\kappa)}\int_{t_n}^{t_{n+1}} f(t,u(t))dt, \tag{36}$$

where

$$\int_{t_n}^{t_{n+1}} f(t,u(t))dt = \int_{t_n}^{t_{n+1}}\left\{\frac{f(t_n,u_n)}{h}(t-t_n) - \frac{f(t_{n-1},u_{n-1})}{h}(t-t_{n-1}) + \frac{f(t_{n-2},u_{n-2})}{h}(t-t_n)\right\}dt, \quad \text{[By Lagrange Interpolation]} \tag{37}$$

$$\int_{t_n}^{t_{n+1}} f(t,u(t))dt = \frac{23h}{12}f(t_n,u_n) - \frac{16h}{12}f(t_{n-1},u_{n-1}) + \frac{5h}{12}f(t_{n-2},u_{n-2}). \tag{38}$$

Thus,

$$u(t_{n+1}) - u(t_n) = \frac{1-\kappa}{CF(\kappa)}\{f(t_n,u_n) - f(t_{n-1},u_{n-1})\} + \frac{\kappa h}{12CF(\kappa)}\times \{23f(t_n,u_n) - 16f(t_{n-1},u_{n-1}) + 5f(t_{n-2},u_{n-2})\}, \tag{39}$$

which implies that,

$$u(t_{n+1}) - u(t_n) = \left(\frac{1-\kappa}{CF(\kappa)} + \frac{23\kappa h}{12CF(\kappa)}\right)f(t_n,u_n) - \left(\frac{1-\kappa}{CF(\kappa)} + \frac{16\kappa h}{12CF(\kappa)}\right)\times f(t_{n-1},u_{n-1}) + \frac{5\kappa h}{12CF(\kappa)}f(t_{n-2},u_{n-2}). \tag{40}$$

Hence,

$$u_{n+1} = u_n + \left(\frac{1-\kappa}{CF(\kappa)} + \frac{23\kappa h}{12CF(\kappa)}\right)f(t_n,u_n) - \left(\frac{1-\kappa}{CF(\kappa)} + \frac{16\alpha h}{12CF(\kappa)}\right)\times f(t_{n-1},u_{n-1}) + \frac{5\kappa h}{12CF(\kappa)}f(t_{n-2},u_{n-2}). \tag{41}$$

This is the Adam-Bashforth three-step approach to obtain the fractional derivative of the Caputo Fabrizio formula, where the error term is

$$
\begin{aligned}
E_r &= \frac{\kappa}{CF(\kappa)} \int_0^t \frac{3}{8} f^{(4)}(\tau) h^3 d\tau, \\
\|E_r\|_\kappa &= \frac{\kappa}{CF(\kappa)} \| \int_0^t \frac{3}{8} f^{(4)}(\tau) h^3 \|_\kappa d\tau \\
&\leq \frac{3\kappa h^3}{8CF(\kappa)} \int_0^t \|f^{(4)}(\tau)\|_\kappa d\tau \\
&\leq \frac{3\kappa h^3}{8CF(\kappa)} . T_{max}(\Theta), \qquad (42)
\end{aligned}
$$

where $\Theta = \max \quad \|f^{(4)}(\tau)\|_\kappa$. Therefore, from (41), we have

$$
u(t_{n+1}) = u(t_n) + Af(t_n, u_n) - Bf(t_{n-1}, u_{n-1}) + Cf(t_{n-2}, u_{n-2}), \qquad (43)
$$

where

$$
A = \frac{1-\kappa}{CF(\kappa)} + \frac{23\kappa h}{12CF(\kappa)}, \quad B = \frac{1-\kappa}{CF(\kappa)} + \frac{16\kappa h}{12CF(\kappa)}, \quad C = \frac{5\kappa h}{12CF(\kappa)}.
$$

Thus, we have the following equations,

$$
\begin{aligned}
x(t_{n+1}) &= x(t_n) + Au(t_n, x_n) - Bu(t_{n-1}, x_{n-1}) + Cu(t_{n-2}, x_{n-2}), \qquad (44) \\
y(t_{n+1}) &= y(t_n) + Av(t_n, y_n) - Bv(t_{n-1}, y_{n-1}) + Cv(t_{n-2}, y_{n-2}), \qquad (45) \\
z(t_{n+1}) &= z(t_n) + Aw(t_n, z_n) - Bw(t_{n-1}, z_{n-1}) + Cw(t_{n-2}, z_{n-2}), \qquad (46)
\end{aligned}
$$

where h represents the step size.

At the point (t_n, x_n), the discrete forms of functions u, v, w are determined by the following equations:

$$
\begin{aligned}
u(t_n, x_n) &= rx_n \left(1 - \frac{x_n}{K}\right) - d_1 x_n - q_1 E_1 x_n, \\
v(t_n, x_n) &= sy_n \left(1 - \frac{y_n + z_n}{L}\right) - m_1 y_n - d_2 y_n - c_1 x_n y_n, \\
w(t_n, x_n) &= m_1 y_n \left(1 - \frac{y_n + z_n}{L}\right) - c_2 x_n z_n - q_2 E_2 z_n.
\end{aligned}
$$

At the point (t_{n-1}, x_{n-1}), the discrete forms of functions u, v, w are determined by the following equations:

$$
\begin{aligned}
u(t_{n-1}, x_{n-1}) &= rx_{n-1} \left(1 - \frac{x_{n-1}}{K}\right) - d_1 x_{n-1} - q_1 E_1 x_{n-1}, \\
v(t_{n-1}, x_{n-1}) &= sy_{n-1} \left(1 - \frac{y_{n-1} + z_{n-1}}{L}\right) - m_1 y_{n-1} - d_2 y_{n-1} - c_1 x_{n-1} y_{n-1}, \\
w(t_{n-1}, x_{n-1}) &= m_1 y_{n-1} \left(1 - \frac{y_{n-1} + z_{n-1}}{L}\right) - c_2 x_{n-1} z_{n-1} - q_2 E_2 z_{n-1}.
\end{aligned}
$$

At the point (t_{n-2}, x_{n-2}), the discrete forms of functions u, v, w are determined by the following equations:

$$
\begin{aligned}
u(t_{n-2},x_{n-2}) &= rx_{n-2}\left(1-\frac{x_{n-2}}{K}\right)-d_1x_{n-2}-q_1E_1x_{n-2},\\
v(t_{n-2},x_{n-2}) &= sy_{n-2}\left(1-\frac{y_{n-2}+z_{n-2}}{L}\right)-m_1y_{n-2}-d_2y_{n-2}-c_1x_{n-2}y_{n-2},\\
w(t_{n-2},x_{n-2}) &= m_1y_{n-2}\left(1-\frac{y_{n-2}+z_{n-2}}{L}\right)-c_2x_{n-2}z_{n-2}-q_2E_2z_{n-2}.
\end{aligned}
$$

Inserting the values of u into (44) results in the subsequent equation,

$$
\begin{aligned}
x(t_{n+1})-x(t_n) = {}& \left(\frac{1-\kappa}{CF(\kappa)}+\frac{23\kappa h}{12CF(\kappa)}\right)\left[rx_n\left(1-\frac{x_n}{K}\right)-d_1x_n-q_1E_1x_n\right]\\
&-\left(\frac{1-\kappa}{CF(\kappa)}+\frac{16\kappa h}{12CF(\kappa)}\right)\left[rx_{n-1}\left(1-\frac{x_{n-1}}{K}\right)-d_1x_{n-1}-q_1E_1x_{n-1}\right]\\
&+\frac{5\kappa h}{12CF(\kappa)}\left[rx_{n-2}\left(1-\frac{x_{n-2}}{K}\right)-d_1x_{n-2}-q_1E_1x_{n-2}\right].
\end{aligned}
$$

Inserting the values of v into (45) results in the subsequent equation,

$$
\begin{aligned}
y(t_{n+1})-y(t_n) = {}& \left(\frac{1-\kappa}{CF(\kappa)}+\frac{23\kappa h}{12CF(\kappa)}\right)\left[sy_n\left(1-\frac{y_n+z_n}{L}\right)-m_1y_n-d_2y_n-c_1x_ny_n\right]\\
&-\left(\frac{1-\kappa}{CF(\kappa)}+\frac{16\kappa h}{12CF(\kappa)}\right)\left[sy_{n-1}\left(1-\frac{y_{n-1}+z_{n-1}}{L}\right)-m_1y_{n-1}-d_2y_{n-1}\right.\\
&\left.-c_1x_{n-1}y_{n-1}\right]+\frac{5\kappa h}{12CF(\kappa)}\left[sy_{n-2}\left(1-\frac{y_{n-2}+z_{n-2}}{L}\right)-m_1y_{n-2}\right.\\
&\left.-d_2y_{n-2}-c_1x_{n-2}y_{n-2}\right].
\end{aligned}
$$

Inserting the values of w into (46) results in the subsequent equation,

$$
\begin{aligned}
z(t_{n+1})-z(t_n) = {}& \left(\frac{1-\kappa}{CF(\kappa)}+\frac{23\kappa h}{12CF(\kappa)}\right)\left[m_1y_n\left(1-\frac{y_n+z_n}{L}\right)-c_2x_nz_n-q_2E_2z_n\right]\\
&-\left(\frac{1-\kappa}{CF(\kappa)}+\frac{16\kappa h}{12CF(\kappa)}\right)\left[m_1y_{n-1}\left(1-\frac{y_{n-1}+z_{n-1}}{L}\right)-c_2x_{n-1}z_{n-1}\right.\\
&\left.-q_2E_2z_{n-1}\right]+\frac{5\kappa h}{12CF(\kappa)}\left[m_1y_{n-2}\left(1-\frac{y_{n-2}+z_{n-2}}{L}\right)-c_2x_{n-2}z_{n-2}\right.\\
&\left.-q_2E_2z_{n-2}\right].
\end{aligned}
$$

10 Results and Discussion

Utilizing the Caputo-Fabrizio derivative, we have performed a numerical simulation of the model of fish population dynamics. The system of (16)–(18), as described earlier, is solved using a three-step Adams-Bashforth method [29]. The simulations are implemented in MATLAB with a step size of $h = 0.01$. The parameters employed in the simulation are assumed for illustrative purposes and are confined to biologically feasible ranges. For the numerical scheme presented in this section, the parameter values listed in Table 1 are used.

Table 1: Parameter descriptions and assigned numerical values.

Parameters	Details of the system's parameters	Values
s	intrinsic population growth rate of the prey species	1.00
r	intrinsic population growth rate of the predator species	0.50
L	carrying capacity of prey	500.00
K	carrying capacity of predator	100.00
d_1	natural mortality rate of predator	0.10
d_2	natural mortality rate of immature prey	0.05
E_1	harvesting effort of predator	6.00
E_2	harvesting effort of prey	5.00
q_1	catchability coefficient of predator	0.05
q_2	catchability coefficient of prey	0.06
m_1	maturity rate of prey species	0.30
c_1	predator's functional feeding response to prey population	0.03
c_2	conversion rate of food for the predator	0.02

Initially, we calculate the densities of both the predator and prey populations within the model for a range of fractional order values. The fractional order, denoted by κ, plays a crucial role in incorporating a memory effect into the system. This memory effect has a substantial influence on the behavior and dynamics of the population density for both the predator and prey populations, shaping how these populations interact and evolve over time under different conditions of κ.

Figure 1(a) illustrates the population density of the predator in the fractional fishery model, where $\kappa = 0.6, 0.7, 0.8, 0.9, 1$ represents the fractional order. Figure 1(a) indicates that stronger memory effects (lower κ) enhance early predator growth and help the system stabilize sooner. In contrast, when κ increases, the growth is slower and the equilibrium is delayed.

Figure 1(b) illustrates the density of immature prey population within the fractional model, where $\kappa = 0.6, 0.7, 0.8, 0.9, 1$ represents the fractional order. The biomass of immature prey initially increases, reaches a peak, and then declines over time. This graph shows a decline due to factors like predation, maturation, or resource limitation. Figure 1(b) also indicates that systems with higher κ exhibit slower stabilization of the population. In contrast, lower κ values reflect stronger memory effects in the fractional system, leading to a faster response and early stabilization.

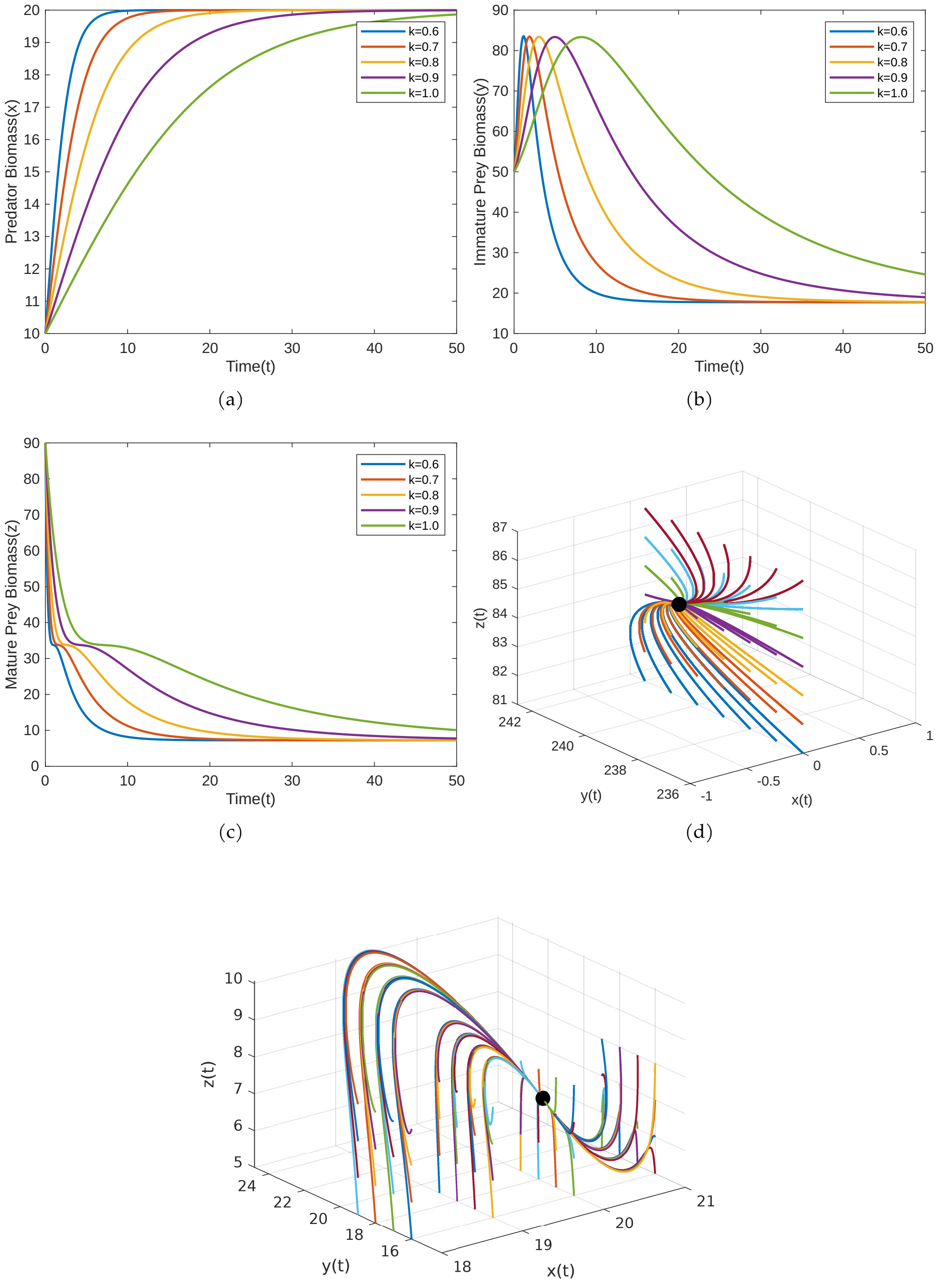

(a) (b)

(c) (d)

(e)

Figure 1: Time series plot of (a) predator population x (b) immature prey population y and (c) mature prey population z with respect to time t for fractional order $\kappa = 0.6, 0.7, 0.8, 0.9, 1$. Phase diagram of the equilibrium point (d) $E_2^*(0, \bar{y}, \bar{z})$ and (e) $E^*(x^*, y^*, z^*)$ for fractional order $\kappa = 0.75$.

Figure 1(c) represents the population density of mature prey within the fractional model with fractional orders $\kappa = 0.6, 0.7, 0.8, 0.9,$ and 1. Figure 1(c) shows that lower values of κ (stronger memory effects) cause the mature prey population to decline more rapidly and stabilize earlier at lower biomass levels. Conversely, higher values of κ leads to slower decline and prolonged persistence of the prey population. This pattern suggests that memory accelerates the impact of predation and harvesting on the mature prey class, making the system more sensitive to past exploitation.

Populations in ecosystems with little or no memory (higher κ) typically react rapidly to disturbances or changes in the environment, which delays their stabilization. Populations react to changes more slowly in ecosystems where memory effects are high (lower κ). Long-term biological processes like delayed reproduction, prolonged maturation times, or environmental factors like resource regeneration could be the cause of this. Over time, the system gradually adapts, resulting in population dynamics that are more sustainable and stable.

Figure 1(d) shows that the absence of predators (or their negligible influence) simplifies the dynamics, focusing only on the interaction between immature and mature prey. The trajectories converge to a stable equilibrium point, representing a balance between immature and mature prey populations without the influence of predators.

Figure 1(e) implies that the inclusion of predator dynamics adds complexity. The trajectories demonstrate oscillatory behavior due to predation and feedback effects between predator and prey populations. The graph represents a stable coexistence equilibrium where predators, immature prey, and mature prey coexist in balance.

11 Conclusions

In this study, we developed and analyzed a mathematical model to explore the dynamics of predator-prey interactions. The study of our predator-prey fractional model highlights the significant role that the fractional order parameter plays in shaping population dynamics. The incorporation of fractional calculus introduces memory effects, which influence how predator and prey populations evolve over time. Our numerical simulations demonstrate that by adjusting the fractional order, we can effectively control the speed at which populations converge toward equilibrium. Specifically, lower fractional orders lead to a more rapid stabilization of the system, while higher fractional orders introduce a delay due to weaker memory effects.

This ability to regulate convergence through fractional-order modeling is crucial for understanding and managing ecological systems. It allows researchers and practitioners to simulate real-world scenarios where species interactions are influenced by past population states and environmental factors. The results indicate that fractional-order models provide a more flexible and accurate representation of predator-prey relationships compared to traditional integer-order models, which assume instantaneous responses to changes.

Overall, our findings underscore the importance of fractional calculus in ecological modeling. This approach provides deeper insights into ecosystem behavior and offers potential applications in ecological conservation, fisheries management, and sustainable harvesting strategies.

Acknowledgement The authors are thankful to the referees for their careful review and meaning-

ful suggestions that improved the manuscript.

Conflicts of Interest The authors declare no conflict of interest.

References

[1] W. Adel, Y. A. Amer, E. S. M. Youssef & A. M. S. Mahdy (2023). Mathematical analysis and simulations for a Caputo-Fabrizio fractional COVID-19 model. *Partial Differential Equations in Applied Mathematics*, *8*, Article ID: 100558. https://doi.org/10.1016/j.padiff.2023.100558.

[2] N. I. Ah, W. M. Kusumawinahyu, A. Suryanto & T. Trisilowati (2023). The dynamics of a predator-prey model involving disease spread in prey and predator cannibalism. *Jambura Journal of Biomathematics*, *4*(2), 119–125. https://doi.org/10.37905/jjbm.v4i2.21495.

[3] E. Ahmed, A. M. A. El-Sayed & H. A. A. El-Saka (2006). On some Routh–Hurwitz conditions for fractional order differential equations and their applications in Lorenz, Rössler, Chua and Chen systems. *Physics Letters A*, *358*(1), 1–4. https://doi.org/10.1016/j.physleta.2006.04.087.

[4] M. B. Almatrafi & M. Berkal (2025). Stability and bifurcation analysis of predator-prey model with Allee effect using conformable derivatives. *Journal of Mathematics and Computer Science*, *36*(3), 299–316. http://dx.doi.org/10.22436/jmcs.036.03.05.

[5] M. B. Almatrafi & M. Berkal (2023). Bifurcation analysis and chaos control for prey-predator model with Allee effect. *International Journal of Analysis and Applications*, *21*, 131–131. https://doi.org/10.28924/2291-8639-21-2023-131.

[6] M. B. Almatrafi & M. Berkal (2025). Bifurcation analysis and chaos control for fractional predator-prey model with Gompertz growth of prey population. *Modern Physics Letters B*, *39*(23), Article ID: 2550103. https://doi.org/10.1142/S0217984925501039.

[7] A. K. Anatoliĭ, H. M. Srivastava & J. J. Trujillo (2006). *Theory and Applications of Fractional Differential Equations*. Elsevier, Amsterdam, Netherlands.

[8] E. Balcı (2023). Predation fear and its carry-over effect in a fractional order prey–predator model with prey refuge. *Chaos, Solitons & Fractals*, *175*, Article ID: 114016. https://doi.org/10.1016/j.chaos.2023.114016.

[9] D. Baleanu, M. H. Abadi, A. Jajarmi, K. Z. Vahid & J. Nieto (2022). A new comparative study on the general fractional model of COVID-19 with isolation and quarantine effects. *Alexandria Engineering Journal*, *61*(6), 4779–4791. https://doi.org/10.1016/j.aej.2021.10.030.

[10] M. Berkal & M. B. Almatrafi (2023). Bifurcation and stability of two-dimensional activator–inhibitor model with fractional-order derivative. *Fractal and Fractional*, *7*(5), Article ID: 344. https://doi.org/10.3390/fractalfract7050344.

[11] B. Bhunia, L. T. Bhutia, T. K. Kar & P. Debnath (2023). Explicit impacts of harvesting on a fractional-order delayed predator–prey model. *The European Physical Journal Special Topics*, *232*(14), 2629–2644. https://doi.org/10.1140/epjs/s11734-023-00941-2.

[12] E. Bonyah, M. L. Juga, C. W. Chukwu & Fatmawati (2022). A fractional order dengue fever model in the context of protected travelers. *Alexandria Engineering Journal*, *61*(1), 927–936. https://doi.org/10.1016/j.aej.2021.04.070.

[13] A. I. K. Butt, W. Ahmad, M. Rafiq, N. Ahmad & M. Imran (2023). Optimally analyzed fractional Coronavirus model with Atangana–Baleanu derivative. *Results in Physics*, *53*, Article ID: 106929. https://doi.org/10.1016/j.rinp.2023.106929.

[14] A. I. K. Butt, M. Imran, K. Azeem, T. Ismaeel & B. A. McKinney (2024). Analyzing HIV/AIDS dynamics with a novel Caputo-Fabrizio fractional order model and optimal control measures. *PLOS One*, *19*(12), Article ID: e0315850. https://doi.org/10.1371/journal.pone.0315850.

[15] M. Caputo & M. Fabrizio (2015). A new definition of fractional derivative without singular kernel. *Progress in Fractional Differentiation & Applications*, *1*(2), 73–85. http://dx.doi.org/10.12785/pfda/010201.

[16] M. Edelman (2013). Fractional maps as maps with power-law memory. In *Nonlinear Dynamics and Complexity*, pp. 79–120. Springer, Cham. https://doi.org/10.1007/978-3-319-02353-3_3.

[17] K. Hattaf (2020). A new generalized definition of fractional derivative with non-singular kernel. *Computation*, *8*(2), Article ID: 49. https://doi.org/10.3390/computation8020049.

[18] L. R. Ibrahim & D. K. Bahlool (2024). Exploring the role of hunting cooperation, and fear in a prey-predator model with two age stages. *Malaysian Journal of Mathematical Sciences*, *18*(4), 727–743. https://doi.org/10.47836/mjms.18.4.03.

[19] M. Javidi & N. Nyamoradi (2013). Dynamic analysis of a fractional order prey–predator interaction with harvesting. *Applied Mathematical Modelling*, *37*(20-21), 8946–8956. https://doi.org/10.1016/j.apm.2013.04.024.

[20] D. Jin & R. Yang (2023). Hopf bifurcation in a predator-prey model with memory effect and intra-species competition in predator. *Journal of Applied Analysis & Computation*, *13*(3), 1321–1335. http://dx.doi.org/10.11948/20220127.

[21] T. K. Kar & K. S. Chaudhuri (2004). Harvesting in a two-prey one-predator fishery: A bioeconomic model. *The ANZIAM Journal*, *45*(3), 443–456. https://doi.org/10.1017/S144618110001347X.

[22] Y. Li, Y. Q. Chen & I. Podlubny (2010). Stability of fractional-order nonlinear dynamic systems: Lyapunov direct method and generalized Mittag–Leffler stability. *Computers & Mathematics with Applications*, *59*(5), 1810–1821. https://doi.org/10.1016/j.camwa.2009.08.019.

[23] J. Losada & J. J. Nieto (2015). Properties of a new fractional derivative without singular kernel. *Progress in Fractional Differentiation and Applications*, *1*(2), 87–92. http://dx.doi.org/10.12785/pfda/010202.

[24] A. J. Lotka (1925). *Elements of Physical Biology*. Williams & Wilkins, Philadelphia, USA. https://doi.org/10.1038/116461b0.

[25] A. Mahata, S. Paul, S. Mukherjee, M. Das & B. Roy (2022). Dynamics of caputo fractional order SEIRV epidemic model with optimal control and stability analysis. *International Journal of Applied and Computational Mathematics*, *8*(1), Article ID: 28. https://doi.org/10.1007/s40819-021-01224-x.

[26] C. Maji (2022). Dynamical analysis of a fractional-order predator–prey model incorporating a constant prey refuge and nonlinear incident rate. *Modeling Earth Systems and Environment*, *8*(1), 47–57. https://doi.org/10.1007/s40808-020-01061-9.

[27] R. Nawaz & N. M. A. Nik Long (2025). System of caputo fractional differential equations for Tuberculosis disease with effects of immune and asymptomatic patients classes: Theoretical and analytical solutions. *Malaysian Journal of Mathematical Sciences*, *19*(2), 443–469. https://doi.org/10.47836/mjms.19.2.05.

[28] Z. M. Odibat & N. T. Shawagfeh (2007). Generalized Taylor's formula. *Applied Mathematics and Computation*, *186*(1), 286–293. https://doi.org/10.1016/j.amc.2006.07.102.

[29] K. M. Owolabi & A. Atangana (2017). Analysis and application of new fractional Adams–Bashforth scheme with Caputo–Fabrizio derivative. *Chaos, Solitons & Fractals*, *105*, 111–119. https://doi.org/10.1016/j.chaos.2017.10.020.

[30] K. M. Owolabi & A. Atangana (2019). On the formulation of Adams–Bashforth method with Atangana–Baleanu–Caputo derivative to model chaotic problems. *Chaos: An Interdisciplinary Journal of Nonlinear Science*, *29*(2), Article ID: 023111. https://doi.org/10.1063/1.5085490.

[31] H. S. Panigoro, A. Suryanto, W. M. Kusumawinahyu & I. Darti (2021). Dynamics of an eco-epidemic predator–prey model involving fractional derivatives with power-law and Mittag–Leffler kernel. *Symmetry*, *13*(5), Article ID: 785. https://doi.org/10.3390/sym13050785.

[32] I. Podlubny (1998). *Fractional Differential Equations: An Introduction To Fractional Derivatives, Fractional Differential Equations, to Methods of Their Solution and Some of Their Applications*. Academic Press, California, USA.

[33] M. Rayungsari, A. Suryanto, W. M. Kusumawinahyu & I. Darti (2023). Dynamics analysis of a predator–prey fractional-order model incorporating predator cannibalism and refuge. *Frontiers in Applied Mathematics and Statistics*, *9*, Article ID: 1122330. https://doi.org/10.3389/fams.2023.1122330.

[34] B. Sahoo & S. Poria (2013). Disease control in a food chain model supplying alternative food. *Applied Mathematical Modelling*, *37*(8), 5653–5663. https://doi.org/10.1016/j.apm.2012.11.017.

[35] N. Sene (2020). Stability analysis of the fractional differential equations with the Caputo-Fabrizio fractional derivative. *Journal of Fractional Calculus and Applications*, *11*(2), 160–172.

[36] Y. Shao & W. Kong (2022). A predator–prey model with Beddington–DeAngelis functional response and multiple delays in deterministic and stochastic environments. *Mathematics*, *10*(18), Article ID: 3378. https://doi.org/10.3390/math10183378.

[37] R. Singh, J. Mishra & V. K. Gupta (2023). Dynamical analysis of a tumor growth model under the effect of fractal fractional Caputo-Fabrizio derivative. *International Journal of Mathematics and Computer in Engineering*, *1*(1), 115–126. http://dx.doi.org/10.2478/ijmce-2023-0009.

[38] A. A. Stanislavsky (2000). Memory effects and macroscopic manifestation of randomness. *Physical Review E*, *61*(5), Article ID: 4752. https://doi.org/10.1103/PhysRevE.61.4752.

[39] A. Suryanto, I. Darti, H. S. Panigoro & A. Kilicman (2019). A fractional-order predator–prey model with ratio-dependent functional response and linear harvesting. *Mathematics*, *7*(11), Article ID: 1100. http://dx.doi.org/10.3390/math7111100.

[40] A. A. Thirthar, S. J. Majeed, M. A. Alqudah, P. Panja & T. Abdeljawad (2022). Fear effect in a predator-prey model with additional food, prey refuge and harvesting on super predator. *Chaos, Solitons & Fractals*, *159*, Article ID: 112091. https://doi.org/10.1016/j.chaos.2022.112091.

[41] M. J. Uddin, S. M. S. Rana, S. Işık & F. Kangalgil (2023). On the qualitative study of a discrete fractional order prey–predator model with the effects of harvesting on predator population. *Chaos, Solitons & Fractals*, *175*, Article ID: 113932. https://doi.org/10.1016/j.chaos.2023.113932.

[42] S. Ullah, M. A. Khan, M. Farooq, Z. Hammouch & D. Baleanu (2020). A fractional model for the dynamics of tuberculosis infection using Caputo-Fabrizio derivative. *Discrete and Continuous Dynamical Systems - S*, *13*(3), 975–993. http://dx.doi.org/10.3934/dcdss.2020057.

[43] M. Vogels, R. Zoeckler, D. M. Stasiw & L. C. Cerny (1975). Pf verhulst's "notice sur la loi que la populations suit dans son accroissement" from correspondence mathematique et physique. ghent, vol. x, 1838. *Journal of Biological Physics*, *3*(4), 183–192. https://doi.org/10.1007/BF02309004.

[44] V. Volterra (1926). *Variazioni e fluttuazioni del numero d'individui in specie animali conviventi*. Società Anonima Tipografica" Leonardo da Vinci", Castello, Italy.

[45] X. Wang, Z. Wang, X. Huang & Y. Li (2018). Dynamic analysis of a delayed fractional-order SIR model with saturated incidence and treatment functions. *International Journal of Bifurcation and Chaos*, *28*(14), Article ID: 1850180. https://doi.org/10.1142/S0218127418501808.